ORIGINAL INNOVATION

Finite element analysis of reinforced concrete curved box-girder bridges

Preeti Agarwal[1]* , Priyaranjan Pal[2] and Pradeep Kumar Mehta[2]

*Correspondence:
gotopreetiagarwal@gmail.com

[1] School of Engineering &
Technology, MUIT Lucknow,
Lucknow 226013, India
[2] Civil Engineering
Department, MNNIT Allahabad,
Prayagraj 211004, India

Abstract

The study presents the design forces of simply supported single-cell reinforced concrete (RC) curved box-girder bridges using a finite element method (FEM) based CSi-Bridge v.20 software. An existing model has been used to validate the present modelling approach. Models subjected to vertical loading, i.e., dead load (DL) and Indian road congress live load (LL), are considered for investigation. An intensive parametric study examines the maximum values of bending moment (BM), shear force (SF), torsional moment (TM), and vertical deflection (VD) in both girders of bridges. The influences of curve angle and span are considered in the study. The effect of curve angle, up to 12°, is negligible on forces and deflections, and thus such bridges can be analysed as a straight one. Finally, non-dimensional equations are derived for evaluating forces and deflections, so that one may predict these quantities for curved bridges based on straight bridge's results. Engineers and designers may consider present work valuable in analysing, and designing curved box-girder bridges.

Keywords: Reinforced concrete, Curve angle, Span length, Indian loading, Finite element method

1 Introduction

Bridges with curved alignment were once uncommon, but the majority of straight bridges have become curved due to site constraints, alignment architecture, traffic volume, and changes in speed limit. The curved box-girder bridge (Fig. 1) has a cellular cross segment that resists the high torsional moment and becomes more efficient. The curved bridge is widely recognized due to its effectiveness, stability, functionality, economy, and aesthetics. These are frequently selected to have a circular plan with transition curves. Analysis of bridges curved in the plan is more complicated than the straight bridges as these are subjected to a combination of bending and torsion induced by girder curvature. Therefore, the section chosen for the design of a curved bridge should have high torsional stiffness to make the section efficient. However, in small curvature bridges, the effect of curve angle on BM, SF, TM, and VD may be neglected if it is within limits. One of the most practiced techniques to analyse and design curved bridges is to treat them straight with defined limitations. In curved bridges, torsion is induced, which affects the response of bridges in flexural, shear, and torsion. It twists the bridge cross-section and produces uneven stresses in the flange. Because of the accessibility of the
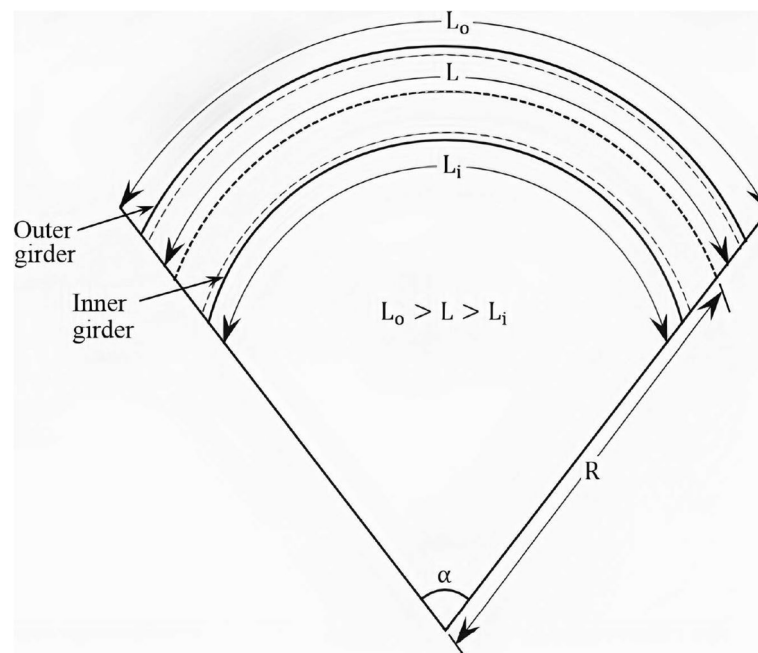
Agarwal *et al. Advances in Bridge Engineering*   (2023) 4:1

Page 2 of 21

Fig. 1 Curved box-girder bridge deck

high-capacity computational system, the analysis and design of curved bridges with more curvature have become easy to deal with.

Many studies have been carried out on curved bridges, and a few of them are included in this paper. Zdenek and Mahjoub (1974) presented the behaviour of straight or curved single-cell box-girder bridges, including longitudinal warping and transverse cross-sectional distortion. Zhang and Lyons (1984) analysed a curved box-girder bridge using thin-walled beam theory and finite element method (FEM). Arizumi et al. (1988) investigated the distortion and slip behaviour of three curved composite box-girder bridges with only end diaphragm experimentally. The effect of curvature and cross-section were considered in the analysis. Sennah and Kennedy (1999) presented the parametric study on a simply supported curved composite multi-cell bridges under the AASTHO (American Association of State Transportation Officials) truck and dead loads, using the finite element method. The bridges were analysed to evaluate the moment, deflection, axial forces, and the results were verified with the experimental results. Aspect ratios, curvature, number of lanes and cells, etc., were considered in the analysis. The authors concluded that increases in the span and degree of curvature increase the moment and deflection distribution factor. Barr et al. (2001) analysed a number of three-span prestressed concrete girder bridges. The effect of lifts, intermediate and end diaphragms, curve angle, etc. on the distribution factors were investigated. Sennah and Kennedy (2001) reviewed and presented some important recommendations for the design of straight and curved box-girder bridges. Sennah and Kennedy (2002) reviewed box-girder bridges, straight and curved, and discussed the behaviour of bridges published in recent literature. The results of box-girder bridges were presented for single-cell, multi-cell, different cross-section, etc. Sennah et al. (2004) presented a method to determine the dynamic impact factors for the horizontally curved composite single or multi-cell

box-girder bridges subjected to the AASTHO truck loadings. DeSantiago et al. (2005) analysed horizontally curved bridges using finite element models considering dead and truck loads. Vertical deflection, bending moment, and torsional moment were determined and compared with the straight bridge and concluded that these are increased with curve angle. The proposed formulae were compared and validated with finite element models and with the specifications of AASTHO. Samaan et al. (Samaan et al., 2007a, b) carried out a dynamic analysis of continuous curved composite multiple-box-girder bridges to determine the natural frequencies and mode shapes using the finite element method. Khaloo and Kafimosavi (2007) studied the flexural behaviour of curved prestressed (post-tensioned) box-girder bridges using the three-dimensional refined finite-element method. The angle of curvature was varied from 0 to 90°, while bridge length, section geometry, and material properties were kept constant. The results of curved bridge were compared with the straight one. Samaan et al. (2007a, b) studied the effect of AASHTO truck load on tangential flexural stresses, deflection, shear forces, and reaction in 180 models of curved continuous composite multiple box-girder bridges. Kim et al. (2007) studied the effect of parameters like curvature, girder spacing, span, and cross-section on the maximum total bending moments in curved bridges to develop a new girder distribution factors (GDF), using numerical methods. The authors concluded that the bending effect on GDFs increases as the span length increases. Fangping and Jianting (2012) investigated the effect of curvature on the deformation of curved bridges due to prestressed tendons, using the finite element based software ANSYS. Five different curved bridges were modelled and analysed to evaluate the mid-span deflections. Cho et al. (2013) presented the distribution of load in straight prestressed concrete (PSC) girder bridges using FEM. The GDF was compared with the AASHTO LRFD, AASHTO standard factors and the finite element analyses results. The formulae were proposed to predict the live load distribution in PSC girder bridges for a preliminary design purpose. Arici et al. (2015) proposed a simple and quick method to evaluate the effect of non-uniform torsion on curved steel girder bridges with box and I-girder cross-sections based on the Hamiltonian structural analysis method. A parametric study was performed on single and multi-span bridges by varying the type of loads, curvature, cross-section, etc. Kumar et al. (2015) investigated the effect of aspect ratio, loading and boundary conditions on the behaviour of bridge. Arici and Granata (2016) proposed an analytical method to evaluate the non-uniform torsional effect in the curved concrete bridge, using the incremental Hamiltonian launching method. The authors studied the effect of secondary torsion on curved bridges. Alawneh et al. (2016) introduced a new framing system with relatively short straight girder segments (6 to 12 m) that are joined and post-tensioned to form a full length curved girder. Majeed et al. (2017) determined the torque behaviour and failure modes of multi-cell box-girder bridge using numerical and experimental methods. Bahadur et al. (2017) investigated the effect of curve angle, span-thickness ratio, and aspect ratio on forces and deflection of simply supported curved rectangular panel. Sali and Mohan (2017) analysed the behaviour of curved trapezoidal bridges and determined the bending stress and displacement along the span length. Androus et al. (2017) presented the elastic and ultimate behaviour of composite box girder bridges experimentally. The effects of cross bracing, curvature, type of loading, etc. are tested on three different composite concrete deck simply supported, two

Agarwal *et al. Advances in Bridge Engineering*   (2023) 4:1

Page 4 of 21

curved and one straight. Shirazi et al. (2018) developed analytical fragility curves for curved single frame concrete box girder bridges with seat-type abutments considering current seismic design considerations as per California Department of Transportation. Said and Khalaf (2018) analysed the horizontally curved box girder bridge under AASTHO loading experimentally and evaluated the live load moment distribution factor. Lalanthi et al. (2018) proposed two methods to determine the stresses and deflection of box-girder bridge using finite element method and found that the results of stresses from the proposed method are lesser than the results obtained from the bending theory. Gupta and Kumar (2018) investigated the flexural behaviour of a simply supported reinforced concrete (RC) skew-curved box-girder bridge using FEM. A new coordinate system for skew-curve was developed to find out the critical position of IRC (Indian Road Congress) Class-70R tracked vehicle loading. The authors concluded that the bending moment in the outer girder of bridge is increased with the curve angle and decreased in the inner girder with the curve angle due to dead and point loads. Gupta et al. (2019a, b) evaluated the fundamental frequency of single, double and triple cells RC curved box-girder bridges using the finite element analysis. Thus, the behaviour of curved RC bridges can be examined using the FEM. Gupta et al. (2019a, b) executed the static analysis of RC curved box-girder bridge using SAP2000 and found that the effect of curve angle less than 12° is insignificant on forces and deflection. Agarwal et al. (2019) investigated the maximum bending moment and shear force in a single-cell skewed box-girder bridge using the finite element analysis. Authors observed the effect of span, girder spacing, and span-depth ratio on the skew box-girder bridge. Agarwal et al. (2020a, b) examined the behaviour of RC skew box-girder bridge subjected to Indian loadings using CSiBridge. Agarwal et al. (Agarwal et al., 2020a, b, Agarwal et al., 2021) studied the combined effect of skew and curve angles on RC box-girder bridges and deduced the force and deflection equations. Mairone et al. (2022) presented a case study on a horizontally curved steel box-girder bridge situated in North Italy using the numerical method. Yuan et al. (2022) determined the mechanical properties and torsional behaviour of curved box-girder bridge. Agarwal et al. (2022a, b) presented the free vibration analysis on different box-girder bridges using the finite element method. Agarwal et al. (2022a, b) presented the modelling of skew, curved and skew-curved bridgea under Indian loading conditions using the numerical method.

The literature mentioned above shows a good amount of study on I-girder and PSC bridges under the AASTHO loading which is different from IRC loading with respect to the load placement and serviceability criteria. Further, it appears that only a little amount of study is available on the Indian standard loading and there are no standard procedures or specifications available in Indian standard Codal provision for curve bridges. Hence, it is important to study the behaviour of box-girder bridge under the IRC loading. The published results available in the literature are useful for the analysis of bridges under the AASTHO truck load which are not useful for the Indian conditions, so in the present study, it is important to focus upon the RC curved bridges, under DL and LL. The goal of the present investigation is to determine the impact of curvature on RC box-girder bridge under IRC loading. The bridges with different degree of complexity can be modelled in easy ways using finite element method. The results obtained from this method are very fast and precise, so becoming quite popular nowadays for the analysis of bridge
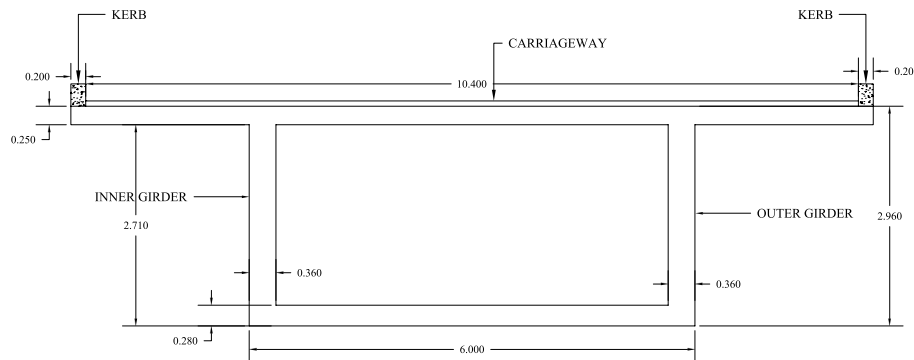
Fig. 2 Validation model of box-girder bridge deck

compared to the experimental methods, which are costly and time consuming. Hence, in the present study, a finite element based software CSiBridge is used for the analysis. The parameters considered in the study are curve angle and span. The effect of these parameters on forces and deflection in both the girders of curved RC box-girder bridge is investigated. The maximum value of forces and deflection are considered for both the girders, not at a particular marked position. For both the girders, several empirical equations are deduced from the statistical approach to determine the bending moment ratio (BMR), shear force ratio (SFR), torsional moment ratio (TMR), and vertical deflection ratio (VDR) for dead as well as live loads. Here, the BMR is the ratio of maximum BM for any curve angle (α) and span (L) to the maximum BM for a straight bridge of 25 m span. Similarly, the other ratios SFR, TMR, and VDR are defined in the present study. Some equations are provided to obtain the combined influence of curve angle and span on the BMR, SFR, TMR, and VDR. These equations are useful for the designers because they can easily analyse the curved bridges with the help of a 25 m span of straight one under the dead and live loads.

2 Modellıng and Valıdatıon

A simply supported RC box-girder bridge situated in China, as shown in Fig. 2, is studied for validation. The left interior support has hinge support, whereas the remaining three supports have roller supports. The same bridge model was considered by Gupta and Kumar (2018) and analysed using a finite element based CSiBridge software. The shell element is used in FE modelling, and each element has four nodes with six degrees of freedom at each node.

The stipulations are: Span = 27.4 m; Width = 10.8 m; Depth (overall) = 2.96 m; Kerb (both sides of deck) = 0.2 m; and thickness of top flange = 250 mm; thickness of bottom flange = 280 mm. The material properties of concrete are: Characteristic strength = 25 MPa; Modulus of elasticity = 2.5×10^4 MPa; Density = 25 kN/m^3 and Poisson's ratio = 0.2.

The box-girder bridge is investigated for DL and LL (Class-70R tracked vehicle, considered as point load). The maximum bending moment (MBM) under dead and live loads in both the girders of the curved deck (curve angle = 0° to 60°) are determined and compared. Figures 3 and 4 demonstrate the maximum bending moment (MBM) under dead and live loads in both the girders of the curved bridge, respectively, having different
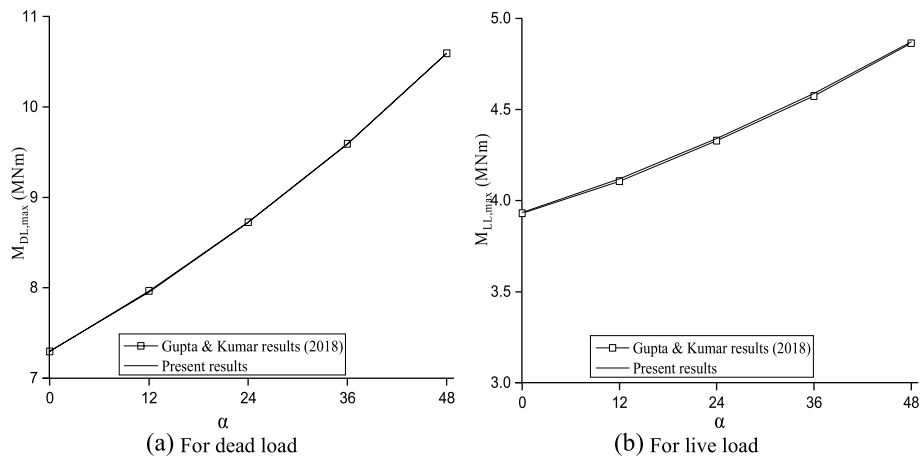
Fig. 3 Variation of MBM with curve angle in outer girder. **a** For dead load. **b** For live load
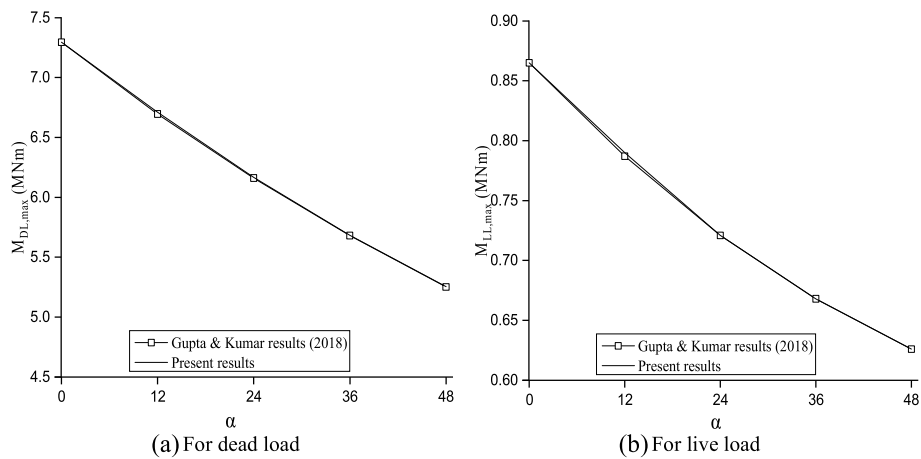

Fig. 4 Variation of MBM with curve angle in inner girder. **a** For dead load. **b** For live load

curve angles. The model and data of Gupta and Kumar (2018) were reproduced/ reconstructed by the authors for validation purposes, and the obtained results are in close agreement with the reported results. Thus, one may say that the present modelling process is acceptable, and it can be extended for further investigation with varying parameters.

3 Results and Discussion

To study the influence of curvature, the behaviour of box-girder bridge deck is investigated for different curve angles and spans. The data considered in the analysis are: Total width = 11.5 m consisting of 7.5 m roadway; Kerb (both sides) = 0.5 m and Footpath (both sides) = 1.5 m. The thickness of top and bottom flanges, and web is assumed to be different for different spans. Figure 5 shows the model of box-girder bridge deck for investigation. The geometric properties of box-girder bridge deck for different spans are listed in Table 1. A trial procedure is used to choose the cross-section. Wherein the depth of the section is determined for a particular span based on an assumed value of
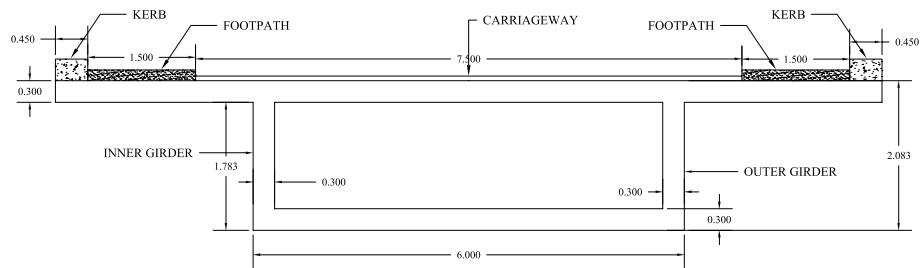
Fig. 5 Model of box-girder bridge deck for present study

Table 1 Geometric properties of single cell box-girder bridge

Properties	Span, L (m)					
	25	30	35	40	45	50
Thickness of top flange, t_{tf} (m)	0.30	0.30	0.30	0.30	0.30	0.30
Thickness of bottom flange, t_{bf} (m)	0.30	0.30	0.32	0.34	0.36	0.38
Thickness of web, t_w (m)	0.30	0.32	0.34	0.36	0.38	0.40
Sectional area, A (m^2)	6.42	6.82	7.37	7.95	8.57	9.24
Moment of inertia, I (m^4)	6.80	10.35	15.16	21.16	28.48	37.26
Section modulus, Z (m^3)	6.74	8.50	10.39	12.38	14.49	16.72

the span to depth ratio (around 10). All straight bridge models are found to be safe under limit states of collapse and serviceability, i.e., stress, deflection, and vibration according to IRC 21:2000. The same cross-sections of straight bridges are used for the investigation of the curved box-girder bridge models. The material properties of concrete used in the models are: Characteristic strength $= 40$ MPa; Modulus of elasticity $= 3.16 \times 10^4$ MPa; Density $= 25$ kN/m³; Poisson's ratio $= 0.2$. The material properties of reinforcing steel are: Modulus of elasticity $= 2 \times 10^5$ MPa; Poisson's ratio $= 0.3$; Density $= 77$ kN/m³; Yield strength $= 500$ MPa; Ultimate tensile strength $= 545$ MPa.

The following are assumed in the analysis: Material is elastic and homogeneous; Deck rests on two longitudinal girders, and the deck is simply supported; Two end diaphragms are provided in all bridge models; intermediate diaphragms are not provided; Footpath and kerb's effects are not considered in all bridge models; other loads such as gravity, wind, seismic, snow, creep, thermal and fatigue are neglected.

All IRC loadings, i.e., Class-70R track and wheel load, Class-AA track and wheel load, and Class-A load (Clause 204.1, IRC 6: 2017), were used to analyse the box-girder bridges. However, only Class-70R track load results are presented here as it produces the most severe stresses and deflection compared to any other IRC loading. Class-70R tracked vehicle consists of two tracks carrying 350 kN load each, which is evenly distributed over a contact area of size 0.84 m × 4.57 m, as shown in Fig. 6 (IRC 6; 2000). This load is positioned 1.2 m away from the kerb to enhance the maximum torsional impact.

The finite element based CsiBridge software has been used to model the deck, including the reinforcement. The deck is discretised with four-noded plate elements, while the reinforcement is for two-noded beam elements. The CsiBridge considers the inbuilt reinforcement based on different codes of practice. The option for inclusion of the specifications contained in clause 16.5.1.1 of IRC: 112–2011 about the minimum longitudinal
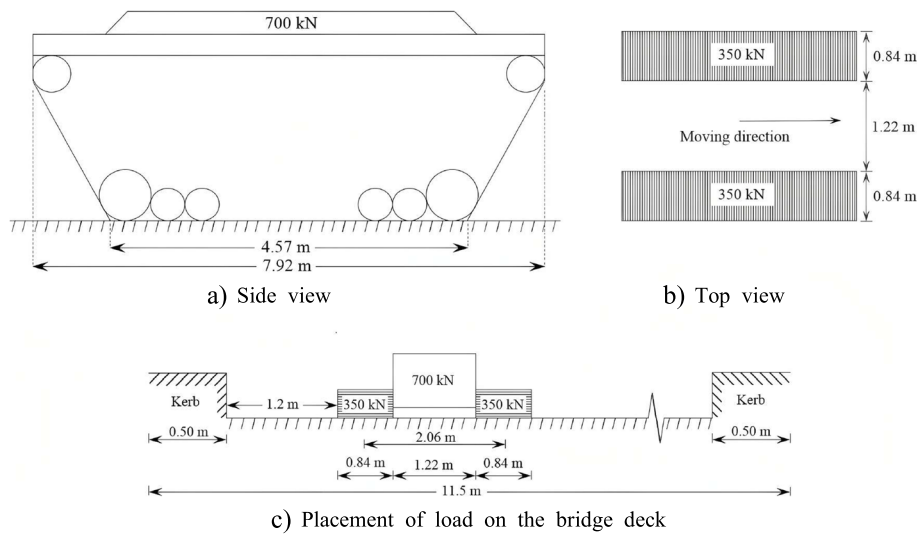
a) Side view   b) Top view

c) Placement of load on the bridge deck

Fig. 6 IRC Class-70R track load. **a** Side view. **b** Top view. **c** Placement of load on the bridge deck

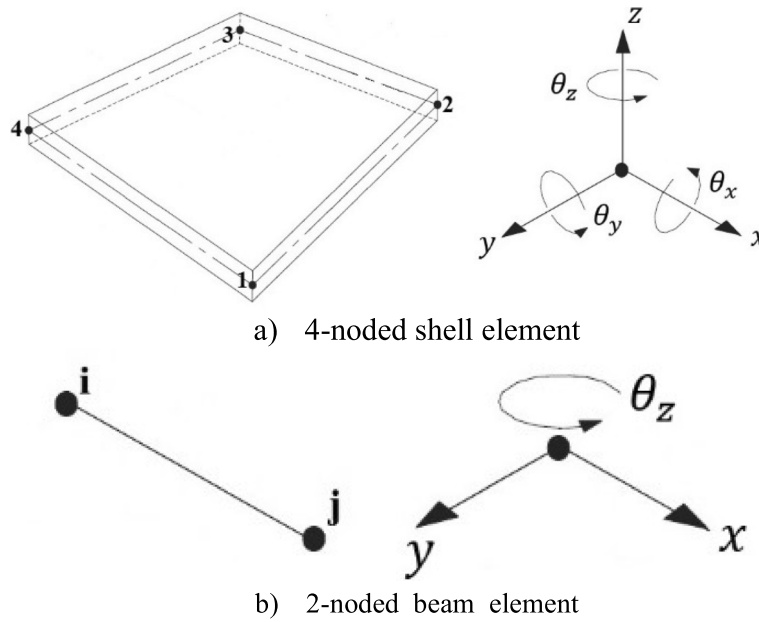a)   4-noded shell element

b)   2-noded beam element

Fig. 7 Description of elements. **a** 4-noded shell element. **b** 2-noded beam element

reinforcement in girder is available in CsiBridge, and thus the same was adopted for the study. Two bearings are placed one under each web at each end of the span for all simply supported bridge models. In the simulation, the bearing at one end of the bridge span is assumed to be roller support, while at other ends, it is considered pin support.

3.1 Description of element

For finite element modelling, the concrete deck and reinforcing bar are discretised using four-noded shell and two-noded beam elements, respectively, as shown in Fig. 7. The shell element has six (three translations and three rotations) degrees of freedom at each node, and the beam element has three (two translations and one rotation) degrees of
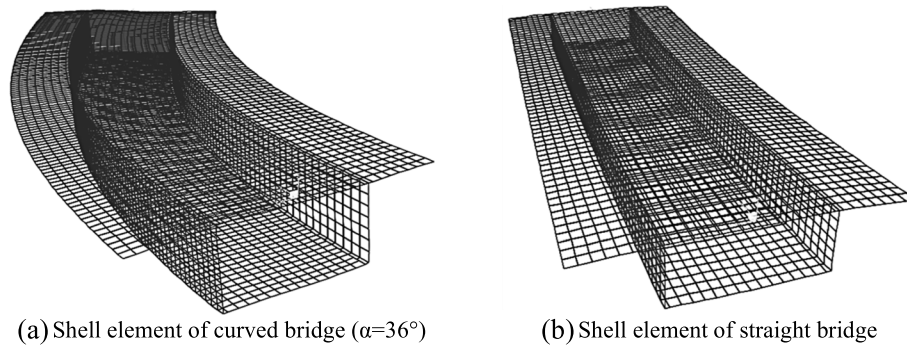
(a) Shell element of curved bridge (α=36°)   (b) Shell element of straight bridge

Fig. 8 Finite element model of box-girder bridge. **a** Shell element of curved bridge (α = 36°). **b** Shell element of straight bridge

Table 2 Convergence study

Mesh Size (mm)	Deflection (mm)
500	9.061
450	9.070
400	9.075
350	9.089
300	9.102
250	9.116
200	9.123
150	9.135
100	9.147
90	9.147
80	9.147

freedom at each node. The used elements' descriptions are extracted from Zienkiewicz et al. (2013) and Seshu (2012).

3.2 Convergence study

A convergence study is carried out to estimate the refinement required to get the closest solution. It specifies the element's size for which the evaluation of the maximum deflection criteria is considered. Models adopted for the analysis are single-cell box-girder bridges, shown in Fig. 8. CSiBridge is widely used to analyse the different types of bridges due to its friendly interface, ease of handling, and computation efficiency. The results are presented in Table 2 and are found to be converged at the mesh size of 100 mm. Hence, 100 mm mesh size is adopted for further parametric study.

3.3 Parametric study

The following parameters, i.e., curve angle and span, are considered for the present parametric study because the curve angle is a crucial parameter in curved bridges, and span directly affects the analysis of bridges. The influence of these parameters on the BM, SF, TM, and VD is studied. The values/ ranges of the parameters stipulated are: Curve
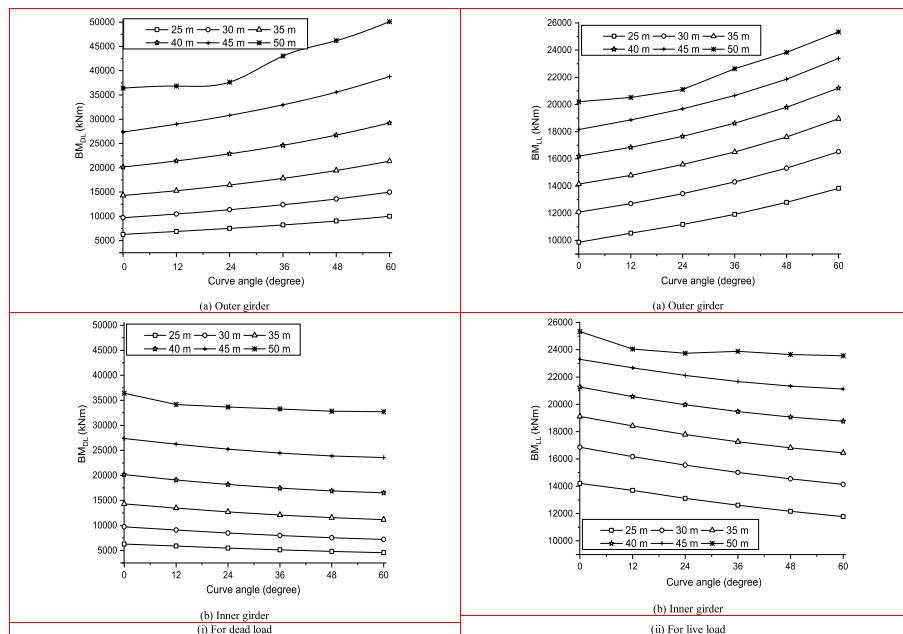
Fig. 9 Variation of bending moment with curve angle for different span. **a** Outer girder. **b** Inner girder. (i) For dead load. (ii) For live load

angle- 0 to 60° at an interval of 12°; and Span- 25 to 50 m, at an interval of 5 m. The influence of different parameters is described separately in the following sections.

3.3.1 Effect of curve angle

The influence of curve angle on maximum values of BM, SF, TM and VD of both the girders (outer and inner) is investigated, separately under both DL and LL. Mostly the box-girder bridge is used for a span 25 m and above due to its beneficial structural behaviour and its intrinsic transverse and torsional rigidity Rajagopalan (2013). In this study, bridge models of 25 to 50 m span with an increment of 5 m having a span-depth ratio (L/d) of 10 with varying curve angles are considered for investigation. Figure 9 depicts the bending moment under DL (BM_{DL}) and bending moment under LL (BM_{LL}) with curve angle for different spans. For outer girder, BM increases considerably with curve angle because of the longer length of the outer girder in comparison to the inner girder. However, it decreases significantly in the case of inner girder. The BM increases significantly with span in both the girders. For outer girder when the curve angle is varied from 0 to 60°, and the span is varied from 25 to 50 m, the BM_{DL} increases by about 1.3 to 1.6 times in comparison to the straight bridge for different spans, while, the respective increase in BM_{LL} lies in the range of about 1.2 to 1.4 times. However, for inner girder, the values decrease, and the respective decrease in BM_{DL} lies in the range of about 1.1 to 1.4 times, while BM_{LL} decreases by about 1.2 times.

Figure 10 illustrates the SF variation along the bridge's outer (longer) and inner (shorter) girders with curve angles for different spans. The SF increases in outer girder significantly with curve angle. While in the inner girder, the shear force under DL (SF_{DL}) decreases with the increase in curve angle (up to 30 m spans) and then increases only for the 60° curve bridge. This typical behavior may occur due to the increased dead load in
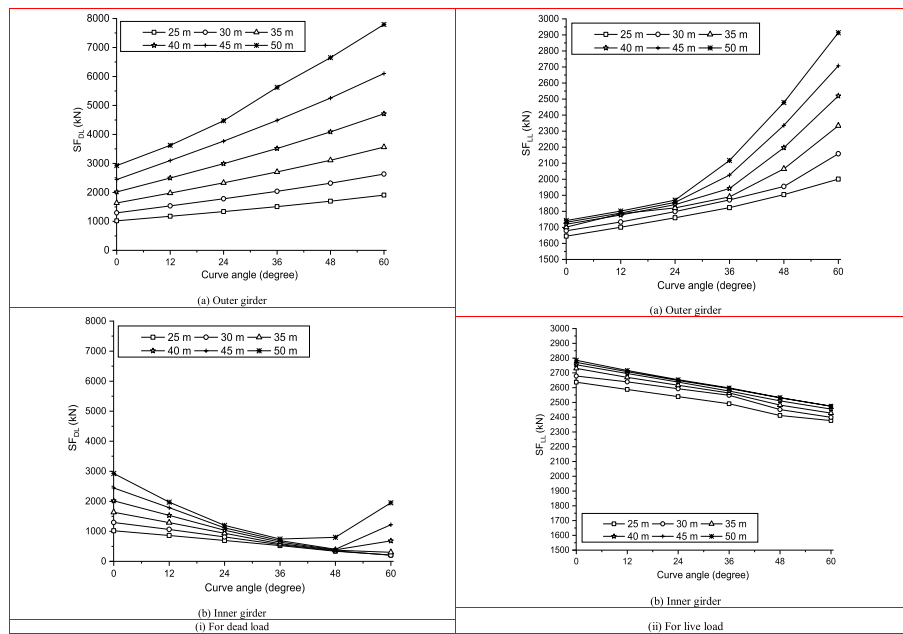
Fig. 10 Variation of shear force with curve angle for different span. **a** Outer girder. **b** Inner girder. (i) For dead load. (ii) For live load

curved bridges with more curvature. Whereas the effect of curve angle on shear force under LL (SF_{LL}) is found to be insignificant. The SF increases significantly with span for both the girders. When the curve angle is varied from 0 to 60°, the increase in SF_{DL} in the outer girder lies in the range of about 1.8 to 2.7 times for different spans compared to the straight bridge, while the SF_{LL} increases in the range of about 1.2 to 1.7 times. For the inner girder, the respective decrease in SF_{DL} lies in between 4.1 to 6.1 times.

The curve angle effect on the TM is shown in Fig. 11. The torsional moment under DL (TM_{DL}) and torsional moment under LL (TM_{LL}) increase in outer girder with curve angle and span. For inner girder up to 30 m span, the TM_{DL} first reduces with increment in curve angle up to 36° and then increases. The span greater than 30 m first reduces with the increment in curve angle up to 24° and then increases. The TM_{LL} in the inner girder is almost unchanged for different spans up to a curve angle of 36°. For the outer girder, when the curve angle is varied from 0 to 60°, increment in TM_{DL} within a range of 2.1 to 4.0 times for different spans and by about 1.4 to 2.5 times in case of TM_{LL}. For the inner girder, the respective increase in TM_{DL} lies in the range of about 1.0 to 3.2 times, while TM_{LL} increases by about 1.0 to 1.9 times.

Figure 12 depicts the variation of VD with curve angle for different spans, under DL and LL. The VD in the outer girder increases with both curve angle and span. It may be due to twisting-induced warping stresses in curved bridges, which increase the deflection. For the inner girder, the vertical deflection under DL (VD_{DL}) increases with span and curve angle; however, VD under LL (VD_{LL}) decreases slightly for all spans up to a curve angle of 36° and then increases. When the curve angle is varied from 0 to 60°, the VD_{DL} in the outer girder increases within a range of about 4.7 to 5.1 times for different spans with respect to the straight bridge, while for VD_{LL} increases in the range of about 4.0 to 4.6 times. For the inner girder, there
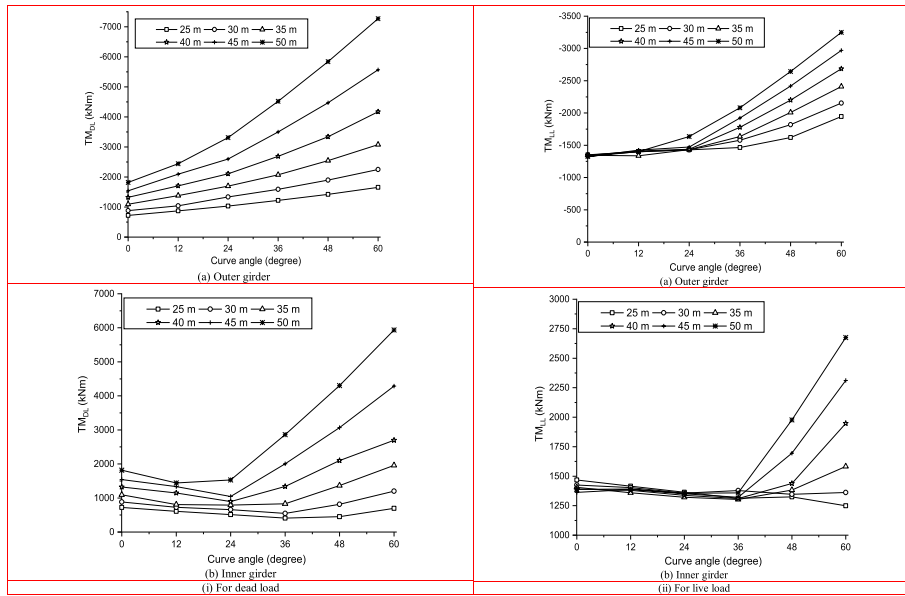
Fig. 11 Variation of torsional moment with curve angle for different span. **a** Outer girder. **b** Inner girder. (i) For dead load. (ii) For live load
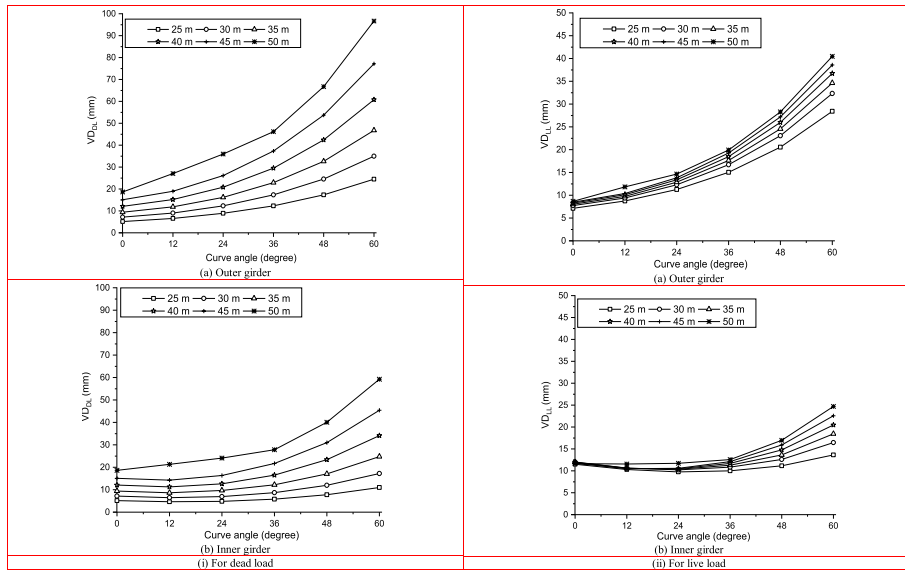

Fig. 12 Variation of vertical deflection with curve angle for different span. **a** Outer girder. **b** Inner girder. (i) For dead load. (ii) For live load

is an increase of about 2.1 to 3.2 times in VD_{DL} values, and the respective increments in VD_{LL} are about 1.2 to 2.1 times.

3.3.2 Effect of span

This section presents the influence of span on the BM, SF, TM, and VD for different curve angles. Figure 13 illustrates the variation of BM for girders with span for different curve angles. It is observed that the effect of curve angle on bending moment
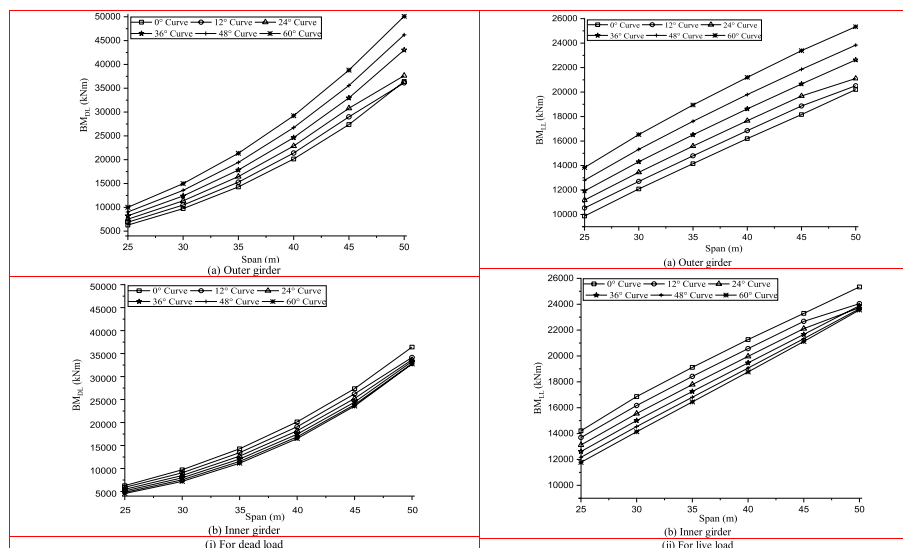
Fig. 13 Variation of bending moment with span for different curve angle. **a** Outer girder. **b** Inner girder. (i) For dead load. (ii) For live load

under DL (BM_{DL}) of both the girders is not much, but it increases slightly with the curve angle; however, the effect of span length is considerable and non-linear. The effect of curve angle on BM_{DL} of the outer girder increases with the span length. The curve angle effect on BM_{DL} is more at the outer girder. The bending moment under live load (BM_{LL}) increases slightly with the curve angle; its variation with span length is significant and almost linear. The effect of curve angle and span length on BM_{LL} is more in the outer girder case, while, in the case of the inner girder, the influence of curve angle is not significant. The influence of the span length on BM_{LL} is much lesser as compared to its effect on BM_{DL}.

For the outer girder, when the span is varied from 25 to 50 m, and the curve angle is increased from 0 to 60°, the BM_{DL} increases within a range of about 5.0 to 5.8 times in comparison to those at 25 m for different curve angles, while for BM_{LL} the respective changes are in the range of about 1.8 to 2.0 times. For the inner girder, there is an increase in BM_{DL} between about 5.8 to 7.2 times, while for BM_{LL}, the increase lies in the range of about 1.7 to 2.0 times.

Figure 14 shows the influence of span on the SF for various curve angles. It is observed that the maximum shear force under DL (SF_{DL}) in both the girders increases with the span length; however, this increment is considerable for the outer girder. The effect of curve angle on SF_{DL} of both the girders is significant, and this increases with span length, being considerably much more in the case of the outer girder.

The maximum shear force under LL (SF_{LL}), in both the girders, increases only slightly with the span length, except in the case of the outer girder for higher curve angles at larger span. The SF_{LL} increases with curve angle in the outer girder, while it decreases for the inner girder. The effect of span length on SF_{LL} is much lesser than that on SF_{DL}. This typical behaviour may occur due to the increased dead load in curved bridges with more curvature. For the outer girder, when the span is varied from 25 to 50 m, the SF_{DL} increases by about 2.8 to 4.0 times compared to those at 25 m for different curve angles.
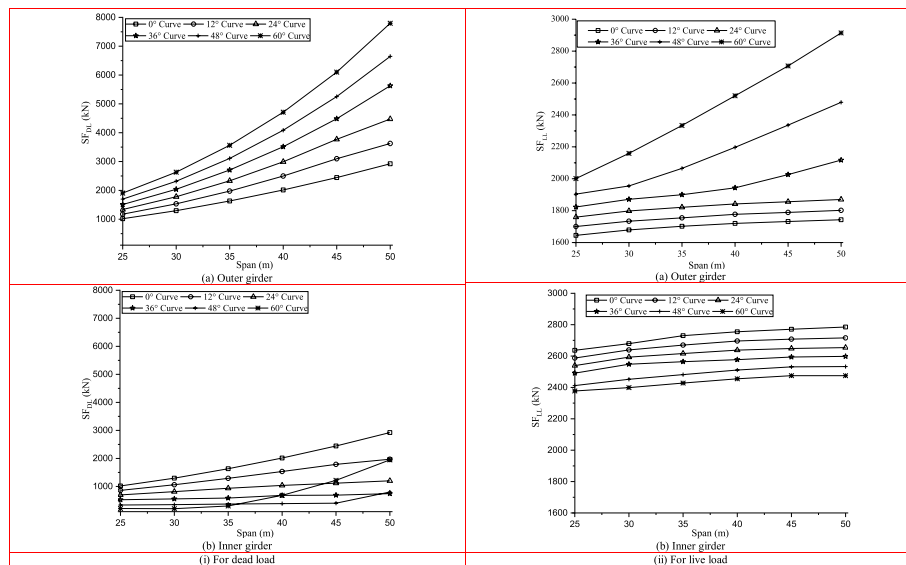
Fig. 14 Variation of shear force with span for different curve angle. **a** Outer girder. **b** Inner girder. (i) For dead load. (ii) For live load
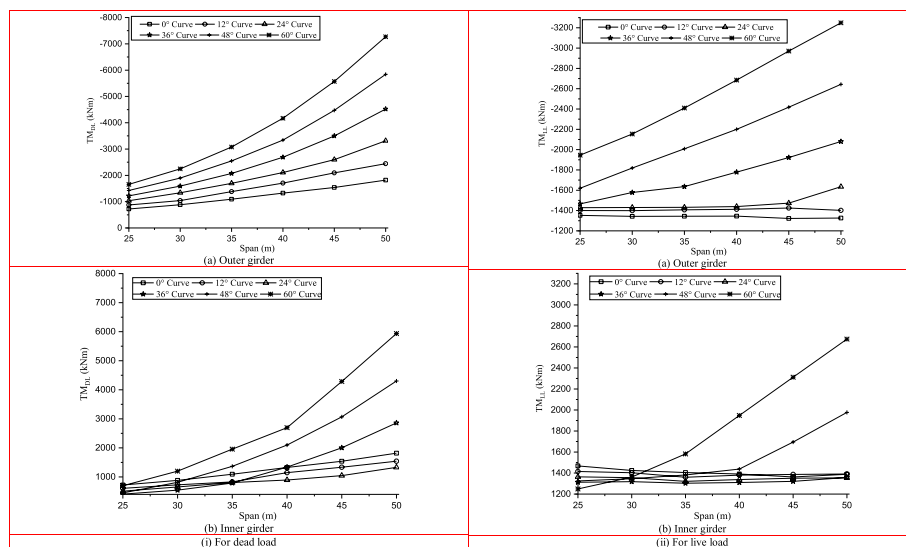

Fig. 15 Variation of torsional moment with span for different curve angle. **a** Outer girder. **b** Inner girder. (i) For dead load. (ii) For live load

While the respective increase in SF_{LL} lies in the range of about 1.0 to 1.45 times. For the inner girder, the respective increase in SF_{DL} lies between about 2.8 to 9.2 times, while the respective increases in SF_{LL} are insignificant.

Figure 15 illustrates the variation of the TM with span for different curve angles for both the girders. It is observed that in both the girders, the maximum torsional moment under DL (TM_{DL}) increases considerably and non-linearly with the span length. The effect of curve angle on TM_{DL} of both the girders increases significantly with the span length and curve angle, especially for the outer girder. The torsional moment ratio under live load (TM_{LL}), in general, increases considerably with the span length for higher curve
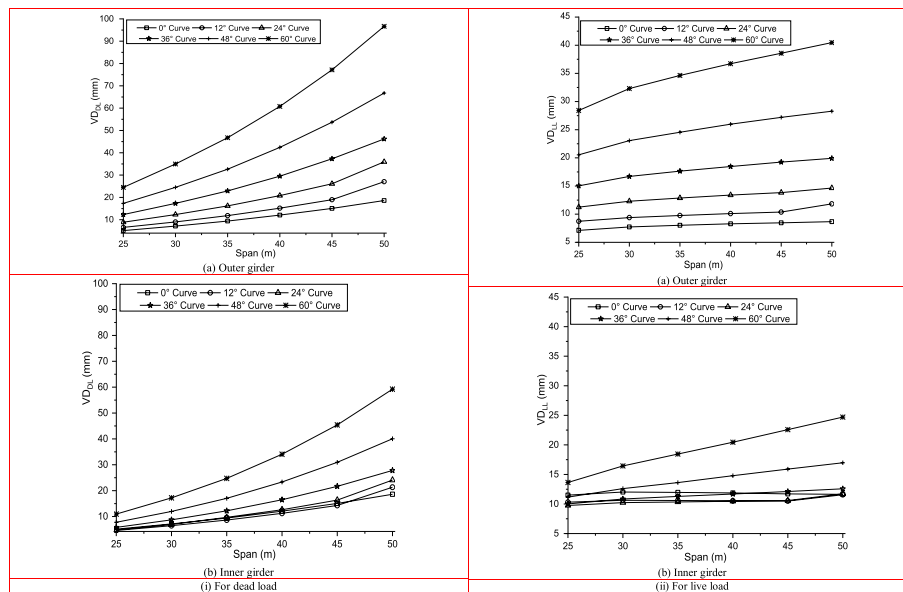
Fig. 16 Variation of vertical deflection with span for different curve angle. **a** Outer girder. **b** Inner girder. (i) For dead load. (ii) For live load

angles, especially in the case of the outer girder. In the outer girder, the effect of span length on TM_{LL} is insignificant up to the curve angle ($\leq 24°$); after that, it increases with curve angle and span length; while for inner girder, the effect of span length on TM_{LL} is insignificant up to the curve angle ($\leq 36°$); after that, it increases with curve angle and span length. This is because of the load placement in higher curved bridges and the twisting induced warping stresses in curved bridges, which increases the torsional moment. The effect of the span length on TM_{DL} is much higher as compared to its effect on TM_{LL}.

For the outer girder when the span is varied from 25 to 50 m, the TM_{DL} increases by about 2.5 to 4.4 times in comparison to those at 25 m for different curve angles, while, the respective increase in TM_{LL} lies in the range of about 1.0 to 1.7 times. However, for the inner girder, the respective increase in TM_{DL} lies between about 2.5 to 9.5 times, while the TM_{LL} increases by about 0.9 to 2.1 times.

Figure 16 shows the variation of VD with span for different curve angles in both girders. The vertical deflection under dead load (VD_{DL}) increases considerably and non-linearly with the span length. In general, the influence of curvature on VD_{DL} of both the girder increases with the span length and curve angle. The effect of curve angle on VD_{DL} of inner girder is not significant up to 24°. The effect of curve angle on VD_{DL} is much higher for the outer girder than the inner girder. The influence of span length on vertical deflection due to live load (VD_{LL}) is not significant up to curve angle 24° for the outer girder, and up to 36° for the inner girder; it increases with the span length and curve angle. However, the effect of span length and curve angle on VD_{LL} is not much in the inner girder, except for the extreme curve angle studied herein. The effect of the span length on VD_{LL} is much lesser as compared to its effect on VD_{DL}.

For the outer girder, when the span is varied from 25 to 50 m, the VD_{DL} increases within a range of about 3.6 to 4.1 times in comparison to those at 25 m span for different curve angles, while for VD_{LL} the respective changes are in the range of about 1.2 to 1.47 times. For the inner girder, there is an increase in VD_{DL} values within a range of about 3.6 to 5.4 times, while for VD_{LL} increases by about 1.0 to 1.8 times.

3.4 Relationship between responses and parameters

A few equations are suggested to obtain the influence of curve angle and span on BMR, SFR, TMR, and VDR in a single cell box-girder bridge. These equations are calculated for both the girders. The two primary loads, namely dead load and IRC Class-70R track load, are considered individually for obtaining the proposed eqs. A statistical approach focused on the least square regression is used for this purpose, utilizing the data collected from the parametric study. The designer may use the proposed equations for estimating the combined effect of curve angle and span while analysing a curved bridge. These equations are valid for the curved bridges of any span subjected to IRC specified loadings. The equations for DL and LL have been presented. To verify the provided equations, some of the BM, SF, TM, and VD results in box-girder bridges, separately for both DL and LL found from the study, are presented in Table 3.

The equations proposed for DL and LL are as follows:

(A) For DL:

- For outer girder, the BMR is

$$BMR_{DL(o)} = 1.01497 + 0.00412L^2 - 0.09223L - 4.2384 \times 10^{-4}L^2 \cos(\alpha) \tag{1}$$

- For inner girder, the BMR is

$$BMR_{DL(i)} = 0.35637 + 4.3234 \times 10^{-5}L^3 - 2.22208 \times 10^{-4}L\alpha \tag{2}$$

- For outer girder, the SFR is

$$SFR_{DL(o)} = 0.44368 + 9.66732 \times 10^{-4}L^2 + 3.69103 \times 10^{-6}L\alpha^2 + 5.48609 \times 10^{-7}\alpha L^3 \tag{3}$$

- For inner girder, the SFR is

$$SFR_{DL}(i) = 661.49711 + 0.06833L + 0.03706\alpha - 0.00206L\alpha - 662.19048\cos\left(1.08418 \times 10^{-8}\ L^2\alpha^2\right) \tag{4}$$

- For outer girder, the TMR is

$$\text{TMR}_{\text{DL(o)}} = 0.05174\,\text{L} + 0.00318\alpha + 1.20542 \times 10^{-8}\alpha\text{L}^4 + 3.34806 \times 10^{-7}\text{L}^2\alpha^2 - 0.23378 \tag{5}$$

- For inner girder, the TMR is

$$\text{TMR}_{\text{DL(i)}} = 0.49536 + 8.09677 \times 10^{-4}\text{L}^2 + 2.25609 \times 10^{-8}\alpha^2\text{L}^3 - 0.0047\alpha - 2.72428 \times 10^{-5}\alpha\text{L}^2 \tag{6}$$

- For outer girder, the VDR is

$$\text{VDR}_{\text{DL(o)}} = 0.66738 + 2.46046 \times 10^{-5}\text{L}^3 + 3.70227 \times 10^{-5}\alpha\text{L}^2 + 1.75834 \times 10^{-8}\alpha^3\text{L}^2 \tag{7}$$

- For inner girder, the VDR is

$$\text{VDR}_{\text{DL(i)}} = 0.51886 + 2.64913 \times 10^{-5}\text{L}^3 + 1.61507 \times 10^{-8}\alpha^3\text{L}^2 - 4.76170 \times 10^{-6}\alpha^3 \tag{8}$$

(B) For LL:

- For outer girder, the BMR is

$$\text{BMR}_{\text{LL(o)}} = 0.04095\text{L} + 0.00440\alpha + 1.62534 \times 10^{-6}\,\text{L}\alpha^2 \tag{9}$$

- For inner girder, the BMR is

$$\text{BMR}_{\text{LL(i)}} = 0.09799 + 0.03819\text{L} - 0.00287\alpha - 8.99692 \times 10^{-5}\text{L}^2 \tag{10}$$

- For outer girder, the SFR is

$$\text{SFR}_{\text{LL(o)}} = 0.97667 + 0.00166\text{L} + 5.75256 \times 10^{-5}\text{L}\alpha + 1.00286 \times 10^{-9}\alpha^3\text{L}^2 \tag{11}$$

- For inner girder, the SFR is

$$\text{SFR}_{\text{LL(i)}} = 0.86067 + 0.00777\text{L} - 0.00188\alpha - 7.90115 \times 10^{-5}\text{L}^2 \tag{12}$$

- For outer girder, the TMR is

Table 3 Verification of the proposed equation

Forces	Girder	Span (m)	Curve angle (degree)	For dead load			For live load		
				Using proposed equation	Using FEM	% variation	Using proposed equation	Using FEM	% variation
BM (kNm)	Outer	30	48	13,811	13,568	1.79	15,314	15,320	0.04
	Inner	30	48	7552	7546	0.08	14,568	14,543	0.17
SF (kN)	Outer	35	24	2305	2331	1.11	1809	1821	0.66
	Inner	35	24	898	935	3.95	2611	2616	0.19
TM (kNm)	Outer	45	60	-5546	-5569	0.41	-2970	-2971	0.03
	Inner	45	60	4291	4287	0.09	2310	2312	0.08
VD (mm)	Outer	40	36	29.23	29.51	0.94	18.35	18.46	0.60
	Inner	40	36	16.43	16.48	0.30	11.66	11.69	0.16

$$\text{TMR}_{\text{LL(o)}} = 0.99411 + 1.15316 \times 10^{-5}L\alpha^2 - 0.00218\alpha - 1.48392 \times 10^{-4}\alpha^2 \quad (13)$$

- For inner girder, the TMR is

$$\text{TMR}_{\text{LL(i)}} = 1.26577 + 1.75345 \times 10^{-4}L^2 + 8.13384 \times 10^{-13}\alpha^4L^3 - 0.01517L \quad - $$
$$8.99448 \times 10^{-5}\alpha^2 \ (14)$$

$$\text{TMR}_{\text{LL(i)}} = 1.26577 + 1.75345 \times 10^{-4}L^2 + 8.13384 \times 10^{-13}\alpha^4L^3 - 0.01517L - 8.99448 \times 10^{-5}\alpha^2$$
$$(14)$$

- For outer girder, the VDR is

$$\text{VDR}_{\text{LL(o)}} = 0.67776 + 0.01791\alpha + 0.012189L + 2.78627 \times 10^{-5}\alpha^2 + 2.17448 \times 10^{-7}L\alpha^3$$
$$(15)$$

- For inner girder, the VDR is

$$\text{VDR}_{\text{LL(i)}} = 1.01571 + 9.13320 \times 10^{-5}\alpha L + 1.39588 \times 10^{-7}\alpha^3L - 0.01093\alpha \quad (16)$$

The values predicted using the proposed equations are also presented in Table 3, along with the percentage error in two values. In all the cases, it is seen that the results deduced from the equations are very close to the finite element analysis results. Thus, the proposed equations may be used to predict the forces and deflection in a curved box-girder bridge with ease.

4 Conclusions

The behaviour of single-cell curved box-girder bridge under dead and live loads were investigated. The parameters that varied were curve angle and span. The following conclusions are drawn based on the obtained results:

- Under DL and LL, the BM increases significantly in the outer girder as the curve angle increases; however, it decreases significantly in the inner girder, whereas the BM increases with span in both girders under dead and live loads. So, the influence of curve angle is greater for the outer girder; hence, one should pay more attention.
- The SF in the outer girder increases significantly with the curve angle under both DL and LL; however, in the case of the inner girder, it reduces as the curve angle increases. The effect of the span is significant on outer girder SF, and it increases with the span, while in the case of the inner girder, the effect is insignificant.
- Under DL and LL, the TM increases in the outer girder as the curve angle increases, while, in the case of the inner girder, it reduces with the increment in curve angle. Under DL and LL, the TM increases with span in the outer girder. In the inner girder, due to DL, TM reduces with the increment in span for up to 24° curvature, and then it increases. But for LL, the TM reduces as the span increases for up to 36° curvature, and then it increases.
- The effect on VD is insignificant up to 35 m span and 24° curve angle, and then it increases with span and curve angle for both girders due to dead and live loads. Up to 24° curvature and 35 m span, the effect is found to be insignificant; thus, these curved bridges may be analysed as similar to straight one.
- The results obtained from the developed equations are quite closer to that obtained from the finite element analysis. So, these equations may directly be used for curved bridges when subjected to both dead load and IRC specified live load.

Abbreviations

$M_{DL,max}$	Maximum dead load bending moment (kNm)
$M_{LL,max}$	Maximum live load bending moment (kNm)
α	Curve angle (degree)
R	Radius of curve bridge (m)
L	Length of central bridge deck (m)
L_o	Length of outer girder bridge deck (m)
L_i	Length of inner girder bridge deck (m)
t_{tf}	Thickness of top flange (m)
t_{bf}	Thickness of bottom flange (m)
t_w	Thickness of web (m)
A	Cross-section area (m^2)
Z	Section modulus of bridge (m^3)
I	Moment of inertia of bridge (m^4)
D	Depth of bridge deck (m)
d	Effective depth of bridge deck (m)
BM_{DL}	Maximum bending moment due to dead load (kNm)
BM_{LL}	Maximum bending moment due to live load (kNm)
SF_{DL}	Maximum shear force due to dead load (kN)
SF_{LL}	Maximum shear force due to live load (kN)
TM_{DL}	Maximum torsional moment due to dead load (kNm)
TM_{LL}	Maximum torsional moment due to live load (kNm)
VD_{DL}	Maximum vertical deflection due to dead load (mm)
VD_{LL}	Maximum vertical deflection due to live load (mm)
$BMR_{DL(o)}$	Bending moment ratio due to dead load for outer girder

$BMR_{DL(i)}$	Bending moment ratio due to dead load for inner girder
$BMR_{LL(o)}$	Bending moment ratio due to live load for outer girder
$BMR_{LL(i)}$	Bending moment ratio due to live load for inner girder
$SFR_{DL(o)}$	Shear force ratio due to dead load for outer girder
$SFR_{DL(i)}$	Shear force ratio due to dead load for inner girder
$SFR_{LL(o)}$	Shear force ratio due to live load for outer girder
$SFR_{LL(i)}$	Shear force ratio due to live load for inner girder
$TMR_{DL(o)}$	Torsional moment ratio due to dead load for outer girder
$TMR_{DL(i)}$	Torsional moment ratio due to dead load for inner girder
$TMR_{LL(o)}$	Torsional moment ratio due to live load for outer girder
$TMR_{LL(i)}$	Torsional moment ratio due to live load for inner girder
$VDR_{DL(o)}$	Vertical deflection ratio due to dead load for outer girder
$VDR_{DL(i)}$	Vertical deflection ratio due to dead load for inner girder
$VDR_{LL(o)}$	Vertical deflection ratio due to live load for outer girder; and
$VDR_{LL(i)}$	Vertical deflection ratio due to live load for inner girder

Declarations

Competing interests
Authors have NO affiliations with or involvement in any organization or entity with any financial interest (such as honoraria; educational grants; participation in speakers' bureaus; membership, employment, consultancies, stock ownership, or other equity interest; and expert testimony or patent-licensing arrangements), or non-financial interest (such as personal or professional relationships, affiliations, knowledge or beliefs) in the subject matter or materials discussed in this manuscript.

References
Agarwal P, Pal P, Mehta PK (2019) Analysis of RC skew box girder bridges. Int J Sci Innov Eng Tech 6:1–8
Agarwal P, Pal P, Mehta PK (2020a) Finite element analysis of skew box-girder bridges. J Struct Eng (Madras) 47(3):1–16 https://serc.res.in/josecontents
Agarwal P, Pal P, Mehta PK (2020) Parametric study on skew-curved RC box-girder bridges. Struct 28:380–388. https://doi.org/10.1016/j.istruc.2020.08.025
Agarwal P, Pal P, Mehta PK (2021) Computation of design forces and deflection in reinforced concrete skew curved box girder bridges. Struct Eng Mech 78(3):255–267. https://doi.org/10.12989/sem.2021.78.3.255
Agarwal P, Pal P, Mehta PK (2022a) Free vibration analysis of RC box-girder bridges using FEM. Sound Vib 56(2):105–125. https://doi.org/10.32604/sv.2022.014874
Agarwal P, Pal P, Mehta PK (2022b) Box-girder bridges - modelling and analysis. Int J Eng Model 35(1):19–42. https://doi.org/10.31534/engmod.2022.1.ri.02m
Alawneh M, Tadros M, Morcous G (2016) Innovative system for curved precast post tensioned concrete I-girder and U-girder bridges. J Bridge Eng ASCE 21(11):1–18. https://doi.org/10.1061/(ASCE)BE.1943-5592.0000938
Androus AA, Afefy HM, Sennah K (2017) Investigation of free vibration and ultimate behavior of composite twin-box girder bridges. J Const Steel Res 130:177–192. https://doi.org/10.1016/j.jcsr.2016.12.017
Arici M, Granata MF (2016) Effects of secondary torsion in curved prestressed concrete bridges built by incremental launching method. Int J Bridge Eng 1–21
Arici M, Granata MF, Oliva M (2015) Influence of secondary torsion on curved steel girder bridges with box and I-girder cross-sections. KSCE J Civ Eng 19:2157–2171. https://doi.org/10.1007/s12205-015-1373-1
Arizumi Y, Hamada S, Oshiro T (1988) Behavior study of curved composite box girders. J Struct Eng ASCE 114(11):2555–2573
Bahadur R, Upadhyay AK, Shukla KK (2017) Static analysis of singly and doubly curved panels on rectangular plan-form. Steel Compos Struct 24(6):659–670. https://doi.org/10.12989/scs.2017.24.6.659

Barr PJ, Eberhard MO, Stanton JF (2001) Live-load distribution factors in prestressed concrete girder bridges. J. Struct. Eng 6(5):298–306. https://doi.org/10.1061/(ASCE)1084-0702(2001)6:5(298)

Cho D, Park S, Kim W (2013) Live load distribution in prestressed concrete girder bridges with curved slab. Appl Mech Mater 284:1441–1445. https://doi.org/10.4028/www.scientific.net/AMM.284-287.1441

CSiBridge Analysis Reference Manual Version 20.0.0, Computers and Structures. Berkeley

DeSantiago E, Mohammadi J, Albaijat HMO (2005) Analysis of horizontally curved bridges using simple finite-element models. Pract. Period. Struct. Des. Constr 10(1):18–21. https://doi.org/10.1061/(ASCE)1084-0680(2005)10:1(18)

Fangping L, Jianting Z (2012) The deformation analysis of the curved box girder bridges under different radius. Mod Appl Sci 6(4):71–76. https://doi.org/10.5539/mas.v6n4p71

Gupta N, Agarwal P, Pal P (2019a) Free vibration analysis of RCC curved box girder bridges. Int J Tech Innov Mod Eng Sci 5:1–7

Gupta N, Agarwal P, Pal P (2019b) Analysis of RCC curved box girder bridges. Appl Innov Res 1:153–159 http://nopr.nisca ir.res.in/handle/123456789/54038

Gupta T, Kumar M (2018) Flexural response of skew-curved concrete box-girder bridges. Eng Struct 163:358–472. https://doi.org/10.1016/j.engstruct.2018.02.063

Indian Road Congress 21 (2000) Standard specification and code of practice for road bridges, section III-cement concrete (plain and reinforced). 3rd edn. New Delhi, India

Indian Road Congress 6 (2016) Standard specification and code of practice for road bridges, section II-loads and stresses. 7th edn. New Delhi, India

Khaloo AR, Kafimosavi M (2007) Enhancement of flexural design of horizontally curved prestressed bridges. J. Bridge Eng 12(5):585–590. https://doi.org/10.1061/(ASCE)1084-0702(2007)12:5(585)

Kim WS, Laman JA, Linzell DG (2007) Live load radial moment distribution for horizontally curved bridges. J. Bridge Eng 12(6):727–736. https://doi.org/10.1061/(ASCE)1084-0702(2007)12:6(727)

Kumar K, Kumar A, Panda SK (2015) Parametric resonance of composite skew plate under non-uniform in-plane loading. Struct Eng Mech 55(2):435–459. https://doi.org/10.12989/sem.2015.55.2.435

Lalanthi MC, Kamatchi PB, Saibhau RK, S. (2018) Methodologies for numerical modelling of prestressed concrete box-girder for long term deflection. Comput Concr 21(3):269–278. https://doi.org/10.12989/cac.2018.21.3.269

Mairone M, Asso R, Masera D, Palumbo P (2022) Behaviour and analysis of horizontally curved steel box-girder bridges. Open J Civ Eng 12(3):390–414. https://doi.org/10.4236/ojce.2022.123022

Majeed AA, Allawi AA, Chai KH, Badaruzzm HWN (2017) Behavior of CFRP strengthened RC multicell box girders under torsion. Struct Eng Mech 61(3):397–406. https://doi.org/10.12989/sem.2017.61.3.397

Rajagopalan N (2013) Bridge Superstructure. Narosa Publishing House, New Delhi

Said A, Khalaf H (2018) Experimental study for horizontally curved box girder bridges with special reference to the live load moment distribution factor. J. Assoc. Arab Univ. Basic Appl Sci 25(3):200–215

Sali J, Mohan RP (2017) Parametric study of single cell box girder bridge under different radii of curvature. Appl Mech Mater 857:165–170. https://doi.org/10.4028/www.scientific.net/AMM.857.165

Samaan M, Kennedy JB, Sennah K (2007) Dynamic analysis of curved continuous multiple-box girder bridges. J. Bridge Eng 12(2):184–193. https://doi.org/10.1061/(ASCE)1084-0702(2007)12:2(184)

Samaan M, Kennedy JB, Sennah K (2007) Impact factors for curved continuous composite multiple-box girder bridges. J. Bridge Eng 12(1):80–88. https://doi.org/10.1061/(ASCE)1084-0702(2007)12:1(80)

Sennah K, Kennedy JB (1999) Simply supported curved cellular bridges: simplified design method. J. Struct. Eng 4(2):85–94. https://doi.org/10.1061/(ASCE)1084-0702(1999)4:2(85)

Sennah KM, Kennedy JB (2001) State-of-the-art in design of curved box-girder bridges. J. Bridge Eng 6(3):159–167. https://doi.org/10.1061/(ASCE)1084-0702(2001)6:3(159)

Sennah KM, Kennedy JB (2002) Literature review in analysis of box-girder bridges. J. Bridge Eng 7(2):134–143. https://doi.org/10.1061/(ASCE)1084-0702(2002)7:2(134)

Sennah KM, Zhang X, Kennedy JB (2004) Impact factors for horizontally curved composite box girder bridges. J. Bridge Eng 9(6):512–520. https://doi.org/10.1061/(ASCE)1084-0702(2004)9:6(512)

Seshu P (2012) Textbook of finite element analysis, 1st edn. PHI Learning Pvt. Ltd., New Delhi

Shirazi RS, Pekcan G, Itani A (2018) Analytical fragility curves for a class of horizontally curved box-girder bridges. J Earthq Eng 22(5):881–901. https://doi.org/10.1080/13632469.2016.1264325

Yuan J, Luo LZ, Yu Y, Shi S, Wang J, Shen J, J. (2022) Analysis of the working performance of large curvature prestressed concrete box girder bridges. Mater 15:1–30. https://doi.org/10.3390/ma15155414

Zdenek PB, Mahjoub EN (1974) Stiffness method for curved box girders at initial stress. J. Struct. Div 100:2070–2090

Zhang SH, Lyons LPR (1984) A thin-walled box beam finite element for curved bridge analysis. Comput Struct 18(6):1035–1046. https://doi.org/10.1016/0045-7949(84)90148-2

Zienkiewicz OC, Taylor RL, Zhu JZ (2013) The finite element method: its basis and fundamentals, 7th edn. Butterworth-Heinemann, United Kingdom

Publisher's Note